

UNCLASSIFIED: Dist A. Approved for public release



Advanced Functionally Graded Plate-Type Structures Impacted By Blast Loading

Terry Hause, Ph.D.

Research Mechanical Engineer

U.S. Army RDECOM-TARDEC, Warren, MI 48397

Report Documentation Page				Form Approved OMB No. 0704-0188	
Public reporting burden for the collection of information is estimated to average 1 hour per response, including the time for reviewing instructions, searching existing data sources, gathering and maintaining the data needed, and completing and reviewing the collection of information. Send comments regarding this burden estimate or any other aspect of this collection of information, including suggestions for reducing this burden, to Washington Headquarters Services, Directorate for Information Operations and Reports, 1215 Jefferson Davis Highway, Suite 1204, Arlington VA 22202-4302. Respondents should be aware that notwithstanding any other provision of law, no person shall be subject to a penalty for failing to comply with a collection of information if it does not display a currently valid OMB control number.					
1. REPORT DATE 05 AUG 2010		2. REPORT TYPE N/A		3. DATES COVERED -	
4. TITLE AND SUBTITLE Advanced Functionally Graded Plate-Type Structures Impacted By Blast Loading				5a. CONTRACT NUMBER	
				5b. GRANT NUMBER	
				5c. PROGRAM ELEMENT NUMBER	
6. AUTHOR(S) Terry Hause, Ph.D.				5d. PROJECT NUMBER	
				5e. TASK NUMBER	
				5f. WORK UNIT NUMBER	
7. PERFORMING ORGANIZATION NAME(S) AND ADDRESS(ES) US Army RDECOM-TARDEC 6501 E 11 Mile Rd Warren, MI 48397-5000, USA				8. PERFORMING ORGANIZATION REPORT NUMBER 21050	
9. SPONSORING/MONITORING AGENCY NAME(S) AND ADDRESS(ES) US Army RDECOM-TARDEC 6501 E 11 Mile Rd Warren, MI 48397-5000, USA				10. SPONSOR/MONITOR'S ACRONYM(S) TACOM/TARDEC	
				11. SPONSOR/MONITOR'S REPORT NUMBER(S) 21050	
12. DISTRIBUTION/AVAILABILITY STATEMENT Approved for public release, distribution unlimited					
13. SUPPLEMENTARY NOTES Presented at NDIAs Ground Vehicle Systems Engineering and Technology Symposium (GVSETS), 17 22 August 2009, Troy, Michigan, USA, The original document contains color images.					
14. ABSTRACT					
15. SUBJECT TERMS					
16. SECURITY CLASSIFICATION OF:			17. LIMITATION OF ABSTRACT SAR	18. NUMBER OF PAGES 39	19a. NAME OF RESPONSIBLE PERSON
a. REPORT unclassified	b. ABSTRACT unclassified	c. THIS PAGE unclassified			



Acknowledgements



The author would like to express thanks to the U.S. Army RDECOM TARDEC for their support and funding under the Independent Laboratory In-House Research Program (ILIR).


UNCLASSIFIED: Dist A. Approved for public release



Outline

MSTV

MODELING AND SIMULATION, TESTING AND VALIDATION



1. Motivation
2. Basic Assumptions and Preliminaries
3. Types of FGM Models
4. Theoretical Developments
5. Solution Methodology
6. Blast Loading
7. Results
8. Conclusions

UNCLASSIFIED: Dist A. Approved for public release

1. Motivation



- A longer service life of the structure operating in extreme environments consisting of severe thermal and mechanical loading conditions.
- Combine the properties of two dissimilar Materials
- The load carrying capacity of plate-type structure is enhanced.
- An increased operational life of the structure.

UNCLASSIFIED: Dist A. Approved for public release

2. Basic Assumptions and Preliminaries

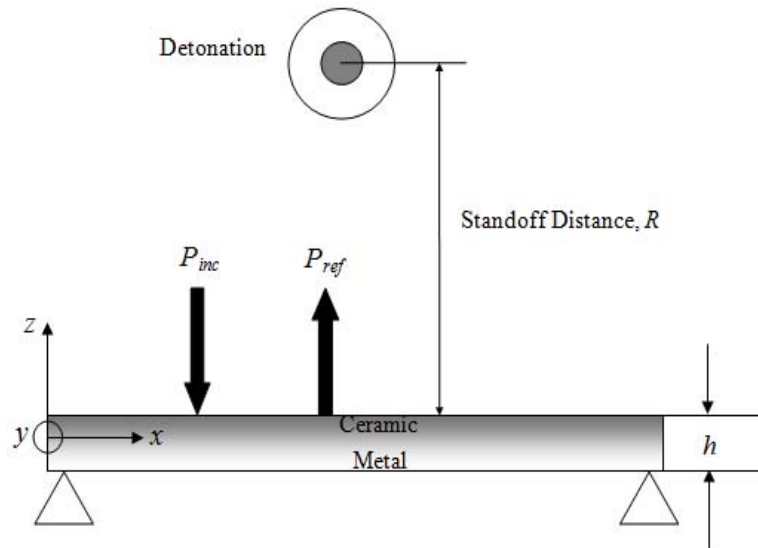


Figure 1. A simply Supported functionally graded (FG) plate shown in 2-D, under an explosive blast

UNCLASSIFIED: Dist A. Approved for public release

2. Basic Assumptions and Preliminaries-Continued



Basic Assumptions

- The plate mid surface is referred to a Cartesian Orthogonal System of Coordinates (x, y, z) .
- Z is the thickness coordinate measured positive in the upwards direction from the mid-surface of the plate with h being the uniform plate thickness.
- The plate is assumed to be thin. As a result, the Kirchhoff Assumptions, of zero transverse shear stresses, will be assumed leading to the classical plate theory.
- The functionally graded plate is composed of ceramic and metal phases whose properties vary smoothly and continuously across the wall thickness from one surface to another.

UNCLASSIFIED: Dist A. Approved for public release

3. Types of FGM Models



Based on a rule of mixtures, the following form of the variation of mechanical properties (Young's Modulus, Density, and Poisson's Ratio) are postulated as

$$P(z) = (P_{\text{ceramic}} - P_{\text{metal}})V_c(z) + P_{\text{metal}}$$

Denotes a Generic Property

Specific Values of the Respective Properties

Volume Fraction

Note : For $V_c(z) = 0$, $P(z) = P_m$ and For $V_c(z) = 1$, $P(z) = P_c$
 $\Rightarrow V_c(z) \in [0,1]$

UNCLASSIFIED: Dist A. Approved for public release

3. Types of FGM Models-Continued

MSTV

MODELING AND SIMULATION, TESTING AND VALIDATION



Type 1: Symmetric Distribution of the Constituent Phases

The phases vary symmetrically through the wall thickness in the sense of having full ceramic at the outer surfaces of the plate and tending toward full metal at the mid-surface

$$V(z, N) = \left(\frac{z}{h/2} \right)^N \frac{1 + \operatorname{sgn} z}{2} + \left(\frac{z}{-h/2} \right)^N \frac{1 - \operatorname{sgn} z}{2}$$

Where,

$$\operatorname{sgn}(z) = \begin{cases} 0, & \text{if } z = 0 \\ -1, & \text{if } z < 0 \\ +1, & \text{if } z > 0 \end{cases} \implies \text{Signum Function}$$

$N \equiv$ Volume Fraction Index ($0 \leq N \leq \infty$)

UNCLASSIFIED: Dist A. Approved for public release

3. Types of FGM Models -Continued

MSTV

MODELING AND SIMULATION, TESTING AND VALIDATION

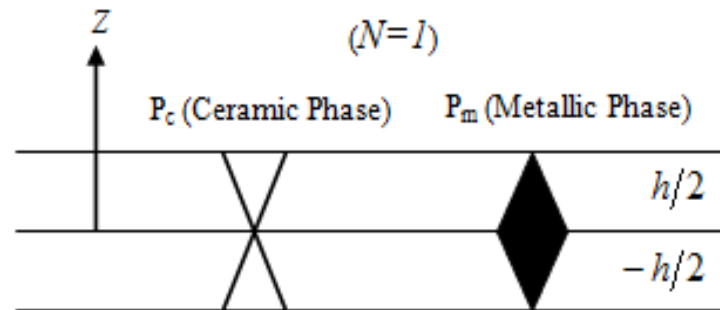


Figure 2. Distribution of the constituent materials through The plate thickness for the symmetric case.

at $z = \pm h/2$, for any N , $V = 1$, and as a result $P(\pm h/2) \Rightarrow P_c$, and for $z = 0$, $V = 0$ and $P(0) \Rightarrow P_m$.

Type 2: Asymmetric Distribution of the Constituent Phases

The phases vary non-symmetrically through the wall thickness and in this case there is Full ceramic at the outer surface of the plate wall and full metal at its inner surface.

UNCLASSIFIED: Dist A. Approved for public release

5 August 2010

9

GVSETS

3. Types of FGM Models-Continued

MSTV

MODELING AND SIMULATION, TESTING AND VALIDATION

$$V(z, N) = [(h - 2z)/2h]^N$$

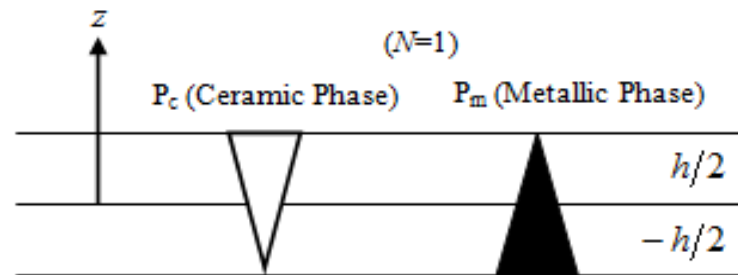
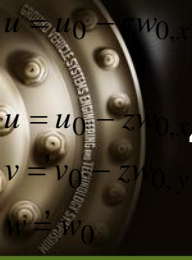


Figure 3. Distribution of the constituent materials through The plate thickness for the asymmetric case.

at $z = +h/2$, $P(h/2) \Rightarrow P_m$, and for $z = -h/2$, $P(-h/2) \Rightarrow P_c$. At the Midsurface, $z = 0$, and for $k = 1$, $P(0) = \frac{1}{2}(P_c + P_m)$

UNCLASSIFIED: Dist A. Approved for public release



4. Theoretical Developments



3-D Displacement Field

$$u(x, y, z, t) = u_0(x, y, t) - z \frac{\partial w_0(x, y, t)}{\partial x}$$

$$v(x, y, z, t) = v_0(x, y, t) - z \frac{\partial w_0(x, y, t)}{\partial y}$$

$$w(x, y, z, t) = w_0(x, y, t)$$

$u_0, v_0, w_0 \Rightarrow$ 2-D displacement quantities of the mid-surface

UNCLASSIFIED: Dist A. Approved for public release

4. Theoretical Developments-Continued



Non-linear Strain-Displacement Relationships

$$\varepsilon_{xx} = \frac{\partial u}{\partial x} + \frac{1}{2} \left(\frac{\partial w}{\partial x} \right)^2$$

$$\varepsilon_{yy} = \frac{\partial v}{\partial y} + \frac{1}{2} \left(\frac{\partial w}{\partial y} \right)^2$$

$$\gamma_{xy} = \frac{\partial u}{\partial y} + \frac{\partial v}{\partial x} + \frac{\partial w}{\partial x} \frac{\partial w}{\partial y}$$

$$\varepsilon_{xz} = \varepsilon_{yz} = \varepsilon_{zz} = 0$$

UNCLASSIFIED: Dist A. Approved for public release

4. Theoretical Developments-Continued

MSTV

MODELING AND SIMULATION, TESTING AND VALIDATION

UNCLASSIFIED: Dist A. Approved for public release

Substitution of the displacement field into the strain-displacement relationships
Gives the 3-D strain measures across the plate thickness as

$$\underbrace{\begin{Bmatrix} \varepsilon_{xx} \\ \varepsilon_{yy} \\ \gamma_{xy} \end{Bmatrix}}_{\{\varepsilon\}} = \underbrace{\begin{Bmatrix} \frac{\partial u_0}{\partial x} + \frac{1}{2} \left(\frac{\partial w_0}{\partial x} \right)^2 \\ \frac{\partial v_0}{\partial y} + \frac{1}{2} \left(\frac{\partial w_0}{\partial y} \right)^2 \\ \frac{\partial u_0}{\partial y} + \frac{\partial v_0}{\partial x} + \frac{\partial w_0}{\partial x} \frac{\partial w_0}{\partial y} \end{Bmatrix}}_{\{\varepsilon^{(0)}\}} + z \underbrace{\begin{Bmatrix} -\frac{\partial^2 w_0}{\partial x^2} \\ -\frac{\partial^2 w_0}{\partial y^2} \\ -\frac{\partial^2 w_0}{\partial x \partial y} \end{Bmatrix}}_{\{\varepsilon^{(1)}\}}$$

3D Strain Measures

2D in-plane strain measures

2D bending Strains

4. Theoretical Developments-Continued



Plane Stress Constitutive Equations

$$\begin{Bmatrix} \sigma_{xx} \\ \sigma_{yy} \\ \sigma_{xy} \end{Bmatrix} = \begin{bmatrix} Q_{11} & Q_{12} & 0 \\ Q_{12} & Q_{22} & 0 \\ 0 & 0 & Q_{66} \end{bmatrix} \begin{Bmatrix} \varepsilon_{xx} \\ \varepsilon_{yy} \\ \gamma_{xy} \end{Bmatrix}$$

$$\sigma_{xz} = \sigma_{yz} = \sigma_{zz} = 0$$

Where,

$$Q_{11} = Q_{22} = \frac{E(z)}{1-\nu^2}, Q_{12} = \frac{\nu E(z)}{1-\nu^2}, Q_{66} = \frac{E(z)}{2(1+\nu)}, Q_{16}, Q_{26} = 0$$

UNCLASSIFIED: Dist A. Approved for public release

4. Theoretical Developments



Governing Equations

$$\int_{t_0}^{t_1} (\delta U + \delta V - \delta K) dt = 0 \Rightarrow \text{Hamilton's Principle}$$

t_0, t_1 are two arbitrary instants in time

U , denotes the strain energy

V , denotes the work done by surface tractions, edge loads, and body forces

K , denotes the kinetic energy of the 3 - D body of the Structure

δ , denotes the variational operator

UNCLASSIFIED: Dist A. Approved for public release

4. Theoretical Developments-Continued

MSTV

MODELING AND SIMULATION, TESTING AND VALIDATION

UNCLASSIFIED: Dist A. Approved for public release



Strain Energy

$$\delta U = \int_{\Omega_0} \int_{-h/2}^{h/2} (\sigma_{xx} \delta \varepsilon_{xx} + \sigma_{yy} \delta \varepsilon_{yy} + \sigma_{xy} \delta \gamma_{xy}) dz d\Omega_0$$

External Work

$$\begin{aligned} \delta V = & - \int_{\Omega_0} P_t(x, y) \delta w \left(x, y, \frac{h}{2} \right) d\Omega_0 - \int_x \int_{-h/2}^{h/2} \left(\sigma_{yy}^* \delta v + \sigma_{yx}^* \delta u \right) dz dx - \\ & \int_y \int_{-h/2}^{h/2} \left(\sigma_{xx}^* \delta u + \sigma_{xy}^* \delta v \right) dz dy \end{aligned}$$

Kinetic Energy

$$\delta K = \int_{\Omega_0} \int_{-h/2}^{h/2} \rho(z) \dot{W} \delta \dot{W} dz d\Omega_0$$

4. Theoretical Developments-Continued



Equations of motion in terms of Stress resultants

$$\frac{\partial N_{xx}}{\partial x} + \frac{\partial N_{xy}}{\partial y} = 0$$

$$\frac{\partial N_{yy}}{\partial y} + \frac{\partial N_{xy}}{\partial x} = 0$$

$$\frac{\partial^2 M_{xx}}{\partial x^2} + 2 \frac{\partial^2 M_{xy}}{\partial x \partial y} + \frac{\partial^2 M_{yy}}{\partial y^2} + \frac{\partial}{\partial x} \left(N_{xx} \frac{\partial w_0}{\partial x} + N_{xy} \frac{\partial w_0}{\partial y} \right) +$$

$$\frac{\partial}{\partial y} \left(N_{yy} \frac{\partial w_0}{\partial y} + N_{xy} \frac{\partial w_0}{\partial x} \right) + P_t - C\dot{w}_0 = I_0 \ddot{w}_0$$

4. Theoretical Developments-Continued



Where,

$$(N_{ij}, M_{ij}) = \int_{-h/2}^{h/2} \sigma_{ij}(1, z) dz \quad (i, j = x, y, xy) \Rightarrow \text{Stress Resultants and Stress Couples}$$

Simply Supported Boundary Conditions

$$w_0 = M_{xx} = N_{xy} = 0, N_{xx} = N_{xx}^* \text{ on } x = 0, L_1$$

$$w_0 = M_{yy} = N_{yx} = 0, N_{yy} = N_{yy}^* \text{ on } y = 0, L_2$$

For Compressive Edge Loading, $N_{xx}^* = -N_{xx}^0$ and $N_{yy}^* = -N_{yy}^0$

5. Solution Methodology



The first two equations of motion are satisfied by assuming the following

$$N_{xx} = \frac{\partial^2 \phi}{\partial y^2}, N_{yy} = \frac{\partial^2 \phi}{\partial x^2}, N_{xy} = -\frac{\partial^2 \phi}{\partial x \partial y}$$

It can be shown, the details of which are not shown here, that the third equation of motion can be expressed in terms of displacements and a stress potential as

$$D \nabla^4 w_0 - \left(\frac{\partial^2 \phi}{\partial x^2} \frac{\partial^2 w_0}{\partial y^2} - 2 \frac{\partial^2 \phi}{\partial x \partial y} \frac{\partial^2 w_0}{\partial x \partial y} + \frac{\partial^2 \phi}{\partial y^2} \frac{\partial^2 w_0}{\partial x^2} \right) + I_0 \ddot{w}_0 + C \dot{w}_0 = P_t$$

UNCLASSIFIED: Dist A. Approved for public release

5. Solution Methodology- Continued



Where,

$$D = \frac{E_1 E_3 - E_2^2}{E_1 (1 - \nu^2)}$$

One more equation in terms of the transversal deflection and the stress potential is needed. This will come from the strain displacement relationships, by eliminating the in-plane displacements, which is known as the compatibility equation which can be shown to be given by

$$\nabla^4 \phi = E_1 \left[\left(\frac{\partial^2 w_0}{\partial x \partial y} \right) - \frac{\partial^2 w_0}{\partial x^2} \frac{\partial^2 w_0}{\partial y^2} \right]$$

5. Solution Methodology- Continued



Where, $\nabla^2 = \frac{\partial^2}{\partial x^2} + \frac{\partial^2}{\partial y^2} \Rightarrow$ Laplacian Operator

Assume a solution form for ϕ, w_0

$$w_0(x, y, t) = w_{mn}(t) \sin \lambda_m x \sin \mu_n y$$

$$\begin{aligned} \phi = & A_{mn}(t) \cos 2\lambda_m x + B_{mn}(t) \cos 2\mu_n y + C_{mn}(t) \cos 2\lambda_m x \cos 2\mu_n y \\ & + D_{mn}(t) \sin 2\lambda_m x \sin 2\mu_n y + \frac{1}{2} N_{xx}^* y^2 + \frac{1}{2} N_{yy}^* x^2 \end{aligned}$$

UNCLASSIFIED: Dist A. Approved for public release

5. Solution Methodology- Continued



Where,

$$\lambda_m = m\pi/L_1, \mu_n = n\pi/L_2, \quad m, n = 1, 2, 3, \dots, \text{etc.}$$

Utilizing the compatibility equation and comparing coefficients gives

$$A_{mn}(t) = \frac{E_1 w_{mn}^2(t) \mu_n^2}{32 \lambda_m^2}, B_{mn}(t) = \frac{E_1 w_{mn}^2(t) \lambda_m^2}{32 \mu_n^2}, C_{mn}(t) = D_{mn}(t) = 0$$

UNCLASSIFIED: Dist A. Approved for public release

5. Solution Methodology- Continued



Transversal Pressure

Let,

$$P_t = P_{mn}(t) \sin \lambda_m x \sin \mu_n y$$

By integrating over the plate area gives

$$P_{mn}(t) = \frac{4}{L_1 L_2} \int_0^{L_2} \int_0^{L_1} P_t(t) \sin \lambda_m x \sin \mu_n y dx dy$$

or

$$P_{mn}(t) = \frac{16 P_t(t)}{\pi^2}, \quad \text{Where, } m, n = 1$$

UNCLASSIFIED: Dist A. Approved for public release

5. Solution Methodology- Continued



Finally, applying the Galerkin method to the third equation of motion Gives the nonlinear equation differential equation governing the Structural response of FG plates under external excitation.

$$\ddot{w}_{mn}(t) + 2\Delta_{mn}\omega_{mn}\dot{w}_{mn}(t) + \omega_{mn}^2 w_{mn}(t) + \Omega_{mn}w_{mn}^3(t) = \tilde{P}_{mn}(t)$$

$w_{mn}(t) \Rightarrow$ Amplitude of Deflection

$\omega_{mn} = \sqrt{K_{mn}/I_0} \Rightarrow$ The natural frequency of the plate

$\Delta_{mn} = C/2I_0\omega_{mn} \Rightarrow$ Nondimensional damping factor

$$\Omega_{mn} = E_1(\lambda_m^4 + \mu_n^4)/16$$

$$\tilde{P}_{mn}(t) = 16P_t(t)/I_0\pi^2$$

UNCLASSIFIED: Dist A. Approved for public release

5. Solution Methodology- Continued



$$K_{mn} = \frac{D\pi^4}{L_1^4} (m^4 + 2m^2n^2\psi^2 + n^4\psi^4) + \frac{N_{xx}^*\pi^2}{L_1^2} (m^2 + n^2\Phi\psi^2)$$

Where,

$\psi = L_1/L_2 \Rightarrow$ Aspect Ratio

$\Phi = N_{yy}^*/N_{xx}^* \Rightarrow$ Compressive/Tensile Edge Load Ratio

The governing nonlinear differential equation is solved using the 4th-Order Runge-Kutta method assuming zero initial conditions.

UNCLASSIFIED: Dist A. Approved for public release

6. Blast Loading

For a free in-air spherical air burst, the pressure profile over time is given in figure 4 as

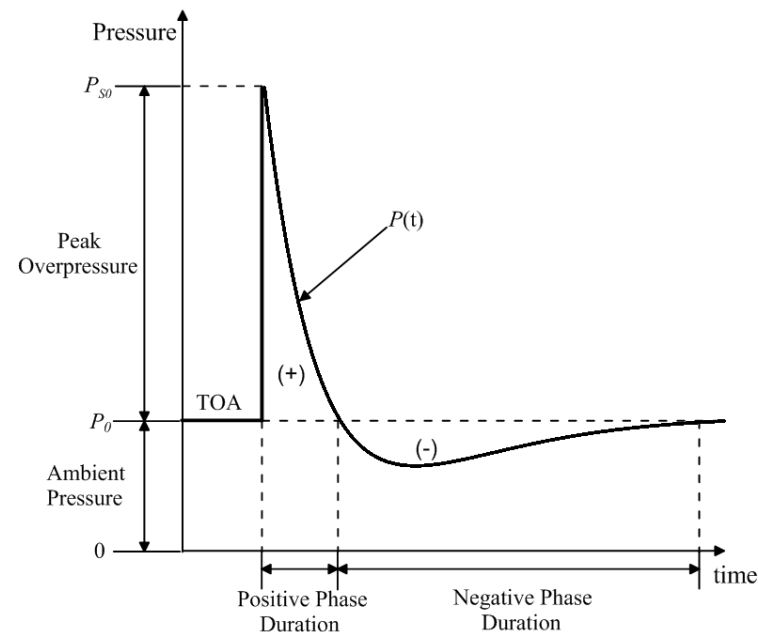


Fig 4. Incident Profile of a blast wave

UNCLASSIFIED: Dist A. Approved for public release

6. Blast Loading-Continued



The wave form shown in figure 4 is given by an expression known as The Friedlander equation and is give as

$$P_t(t) = (P_{so} - P_o) \left(1 - \frac{t - t_a}{t_p} \right) e^{-\alpha \left(\frac{t - t_a}{t_p} \right)}$$

Where,

$$P_{so} = \frac{1772}{Z^3} - \frac{114}{Z^2} + \frac{108}{Z} \Rightarrow \text{Peak Overpressure over ambient}$$

$$Z = R/W^{1/3} \Rightarrow \text{scaled distance} \left\{ \begin{array}{l} R \text{ is the Standoff Distance} \\ W \text{ is the equivalent weight of charge} \\ \text{of TNT in terms of kilograms} \end{array} \right.$$

6. Blast Loading-Continued

MSTV

MODELING AND SIMULATION, TESTING AND VALIDATION

UNCLASSIFIED: Dist A. Approved for public release



P_o is the ambient pressure

t_a is the time of arrival

t_p is the positive phase duration of the blast wave

t is the time

For conditions of STP at sea level, the time of arrival and the positive phase duration can be determined from

Arrival time or positive phase duration

$$\frac{t}{t_1} = \frac{R}{R_1} = \left(\frac{W}{W_1} \right)^{\frac{1}{3}} \Rightarrow \text{Cube root scaling}$$

Arrival time or positive phase duration for a reference explosion of charge weight, W_1

It should be noted that the standoff distances are themselves scaled
According to the cube root law



Validation of the Present Approach

Comparisons are made (Akay, H.U., 1980) who considered explosive blast of Metallic plates under a step loading excitation given by

$$P_t(t) = P[H(t) - H(t - t_0)]$$

$H(t)$ is referred to as the Heaviside Step Function defined as $H(t) = 1$ for $t \geq 0$ and $H(t) = 0$ for $t < 0$

The geometrical and material properties used were

$$L_1 = 2.438m, h = 0.00635m, \psi = 1$$

$$E_m = 70.3GPa, \rho_m = 2547kg/m^3, \nu_{ave} = 0.25$$

7. Results-Continued

MSTV

MODELING AND SIMULATION, TESTING AND VALIDATION

UNCLASSIFIED: Dist A. Approved for public release

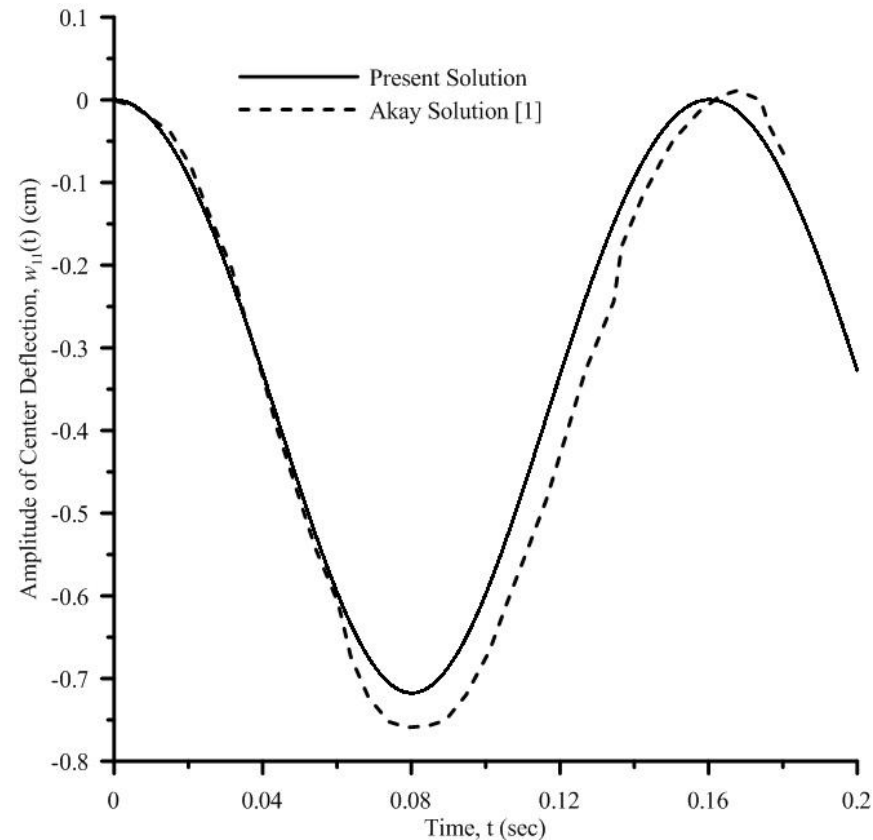


Fig 5. Comparisons of solutions of the time history of the Central deflection Under a Step Load $P = 48.82Pa$, $t_0 = 0.2$ sec

7. Results-Continued



Present Results

A ceramic-metal functionally graded plate with the following properties were used

Table 1. Material Properties

	Metal (Ti-6Al-4V)	Ceramic (Aluminum Oxide)
E , Modulus (GPa)	105.7	320.24
ν , Poisson's Ratio (Unitless)	0.2981	0.26
ρ , Density (Kg/m ³)	4429	3750

($L_1 = 1$ m, $\psi = 1$, $h = 0.0254$ m)

UNCLASSIFIED: Dist A. Approved for public release

7. Results-Continued

MSTV

MODELING AND SIMULATION, TESTING AND VALIDATION



Table 2. Air blast parameters versus distance for a one Kilogram TNT spherical air burst (Kingery and Bulmash, 1984).

Standoff Distance, (m)	Arrival Time, (msec)	Positive Phase Duration, (msec)
1.0	0.532	1.79

UNCLASSIFIED: Dist A. Approved for public release

7. Results-Continued

MSTV

MODELING AND SIMULATION, TESTING AND VALIDATION

UNCLASSIFIED: Dist A. Approved for public release

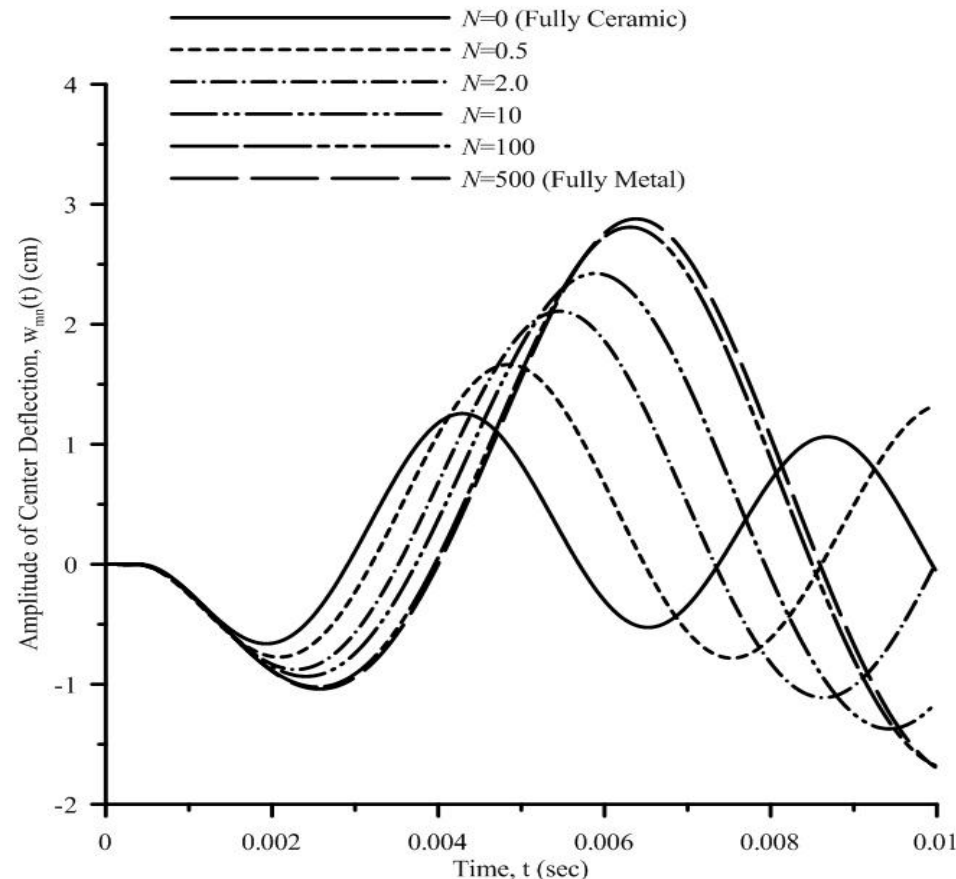


Fig 6. Implications of the volume fraction index on the deflection-time history of an asymmetric FG Plate without damping.

7. Results-Continued

MSTV

MODELING AND SIMULATION, TESTING AND VALIDATION

UNCLASSIFIED: Dist A. Approved for public release

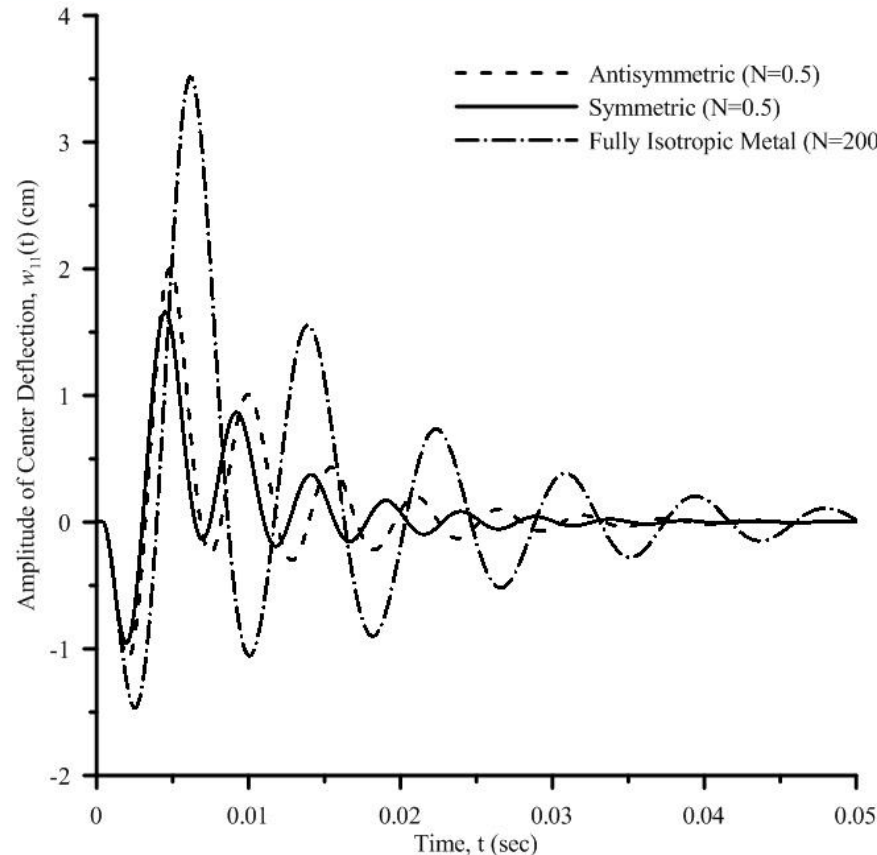


Fig 7. Implications of the symmetry on the deflection-time response of FG plate. $\Delta_{11} = 0.1$

7. Results-Continued

MSTV

MODELING AND SIMULATION, TESTING AND VALIDATION

UNCLASSIFIED: Dist A. Approved for public release

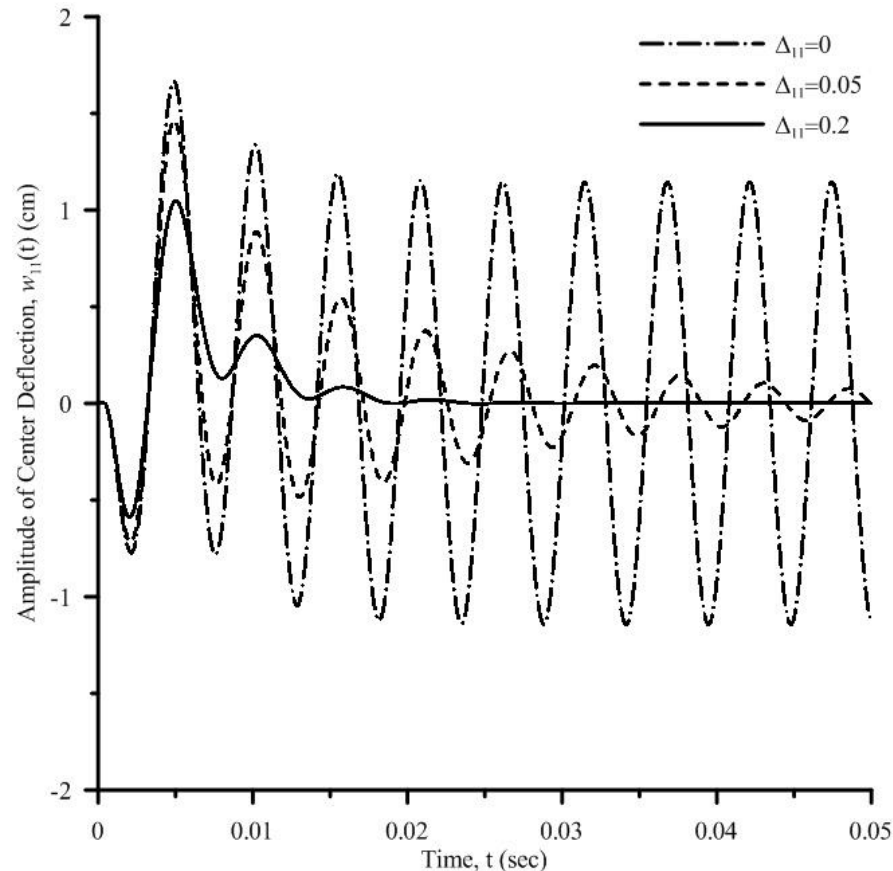


Fig 8. Implications of various amounts of damping on the deflection-time response of an asymmetric FG Plate. ($N=0.5$)

7. Results-Continued

MSTV

MODELING AND SIMULATION, TESTING AND VALIDATION

UNCLASSIFIED: Dist A. Approved for public release

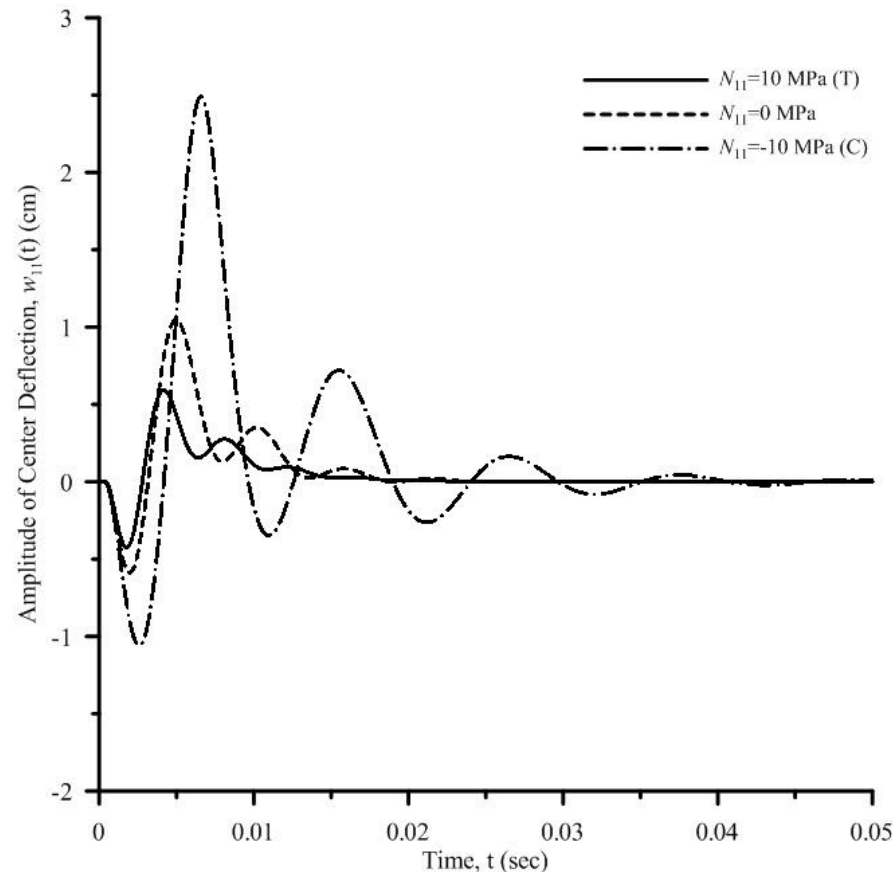


Fig. 9. The implications of the compressive/tensile edge loading on the deflection-time response of an asymmetric FG plate.
($\Delta_{11} = 0.2, N = 0.5$)

7. Results-Continued

MSTV

MODELING AND SIMULATION, TESTING AND VALIDATION

UNCLASSIFIED: Dist A. Approved for public release

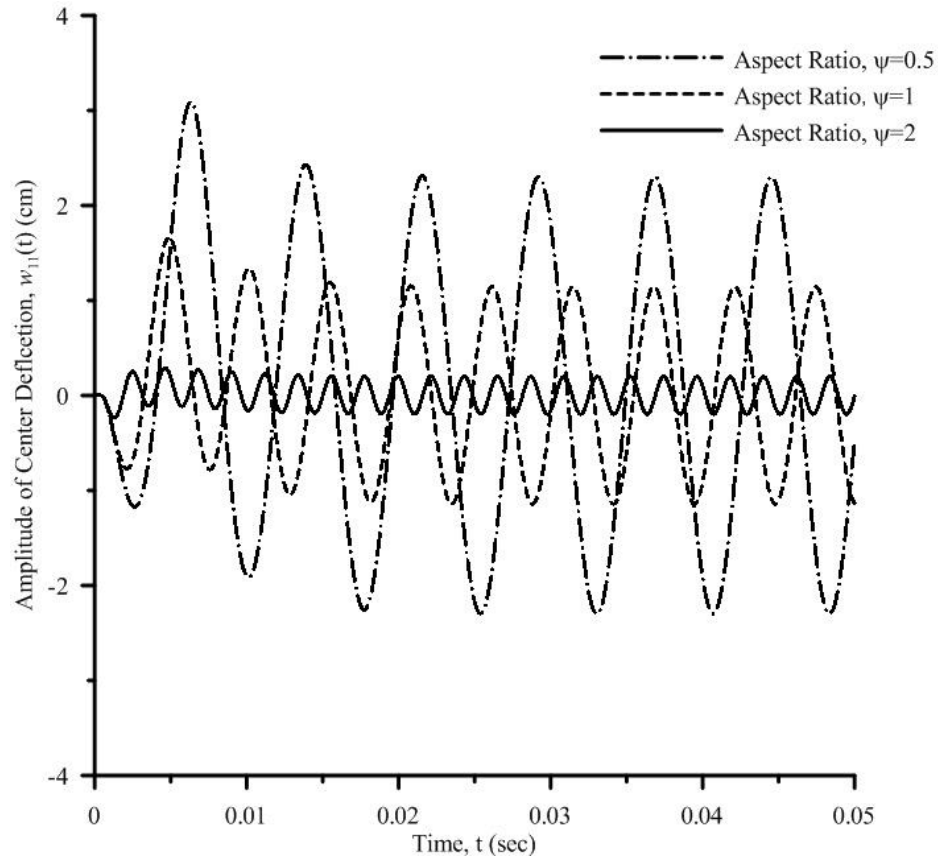


Fig. 10. The effects of various aspect ratios of an asymmetric FG plate on the deflection-time response. ($N=0.5$)

7. Results-Continued

MSTV

MODELING AND SIMULATION, TESTING AND VALIDATION

UNCLASSIFIED: Dist A. Approved for public release

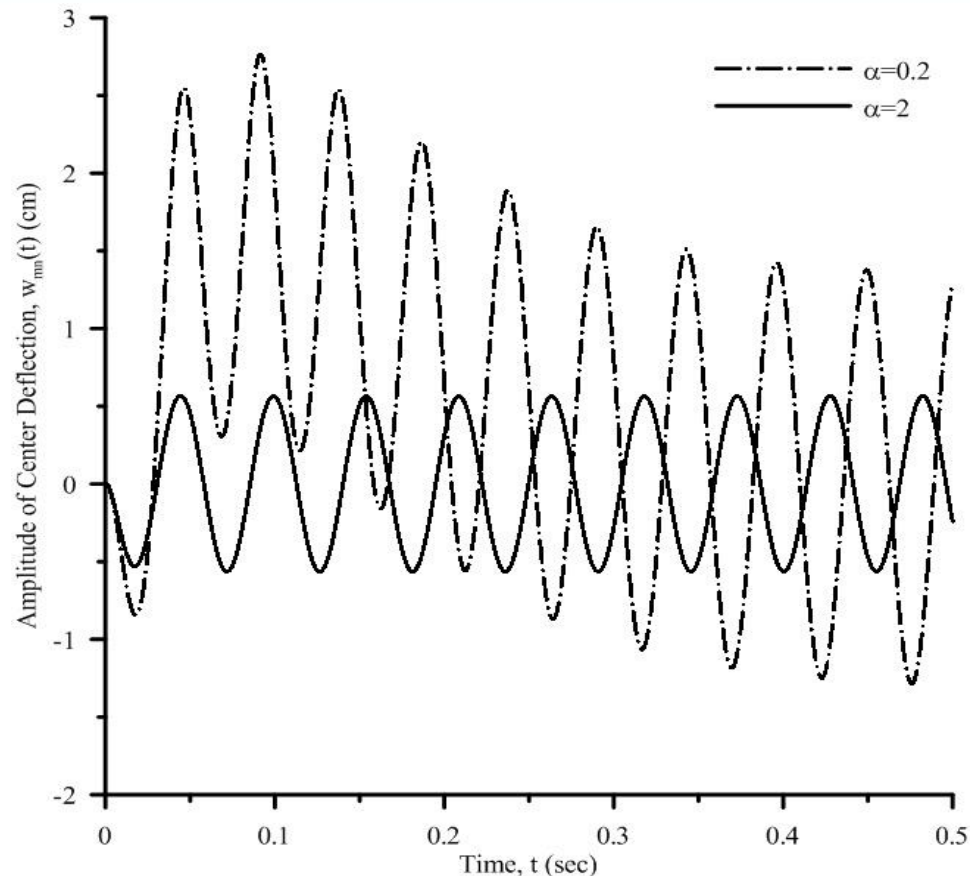


Fig. 11. The implications of the value of the decay parameter on the time-deflection response of a asymmetric FG Plate without damping. ($N=0.5$)

8. Conclusions

MSTV

MODELING AND SIMULATION, TESTING AND VALIDATION

UNCLASSIFIED: Dist A. Approved for public release

- A Structural Model of the dynamic response of functionally graded plates exposed to a free in-air blast with simply supported boundary conditions has been presented.
- As the volume fraction of ceramic increases, the deflections become smaller with higher frequencies in contrast to metal phase.
- The symmetric construction due to being stiffer has smaller deflections and higher frequencies as compared to the asymmetric construction
- For a fixed compressive edge load, as the metal concentration increases, the deflections increase with decreasing frequencies.